Tuned to Perfection: Ironing Out the Defects in Metal-Organic Framework UiO-66

UNIVERSITÀ DEGLI STUDI DI TORINO

G. Shearer, S. Chavan, J. Ethiraj, J. G. Vitillo, S. Svelle, U. Olsbye, C, Lamberti, S. Bordiga, K. P. Lillerud

"Tuned to Perfection: Ironing out the Defects in UiO-66"

Chem. Mater., **26** (2014) 4068-4071

DOI: 10.1021/cm501859p

Tuned to Perfection: Ironing Out the Defects in Metal–Organic Framework UiO-66

Greig C. Shearer†, Sachin Chavan†, Jayashree Ethiraj‡, Jenny G. Vitillo‡, Stian Svelle†, Unni Olsbye†, Carlo Lamberti‡, Silvia Bordiga†‡, and Karl Petter Lillerud*†
† inGAP Centre for Research Based Innovation, Department of Chemistry, University of Oslo, P.O. Box 1033, N-0315 Oslo, Norway
‡ Department of Chemistry, NIS and INSTM Reference Centre, , Via Quarello 15, I-10135 Torino, Italy

*E-mail: k.p.lillerud@kjemi.uio.no.

Metal–organic frameworks (MOFs) are a relatively new class of crystalline porous materials.(1) One family of these materials that has attracted considerable attention due to their high thermal, chemical, and mechanical stability is the zirconium based MOFs of the UiO family.(2) The material with benzene-1,4-dicarboxylic acid (BDC) as linker is named UiO-66 and is considered to be the parent of the series, from which other members are derived via isoreticular synthesis.(2, 3) A multitude of synthetic procedures has been reported for UiO-66, with the majority of groups utilizing their own strategies in favor of using one from the pool of pre-existing protocols.(4) With the exception of two recent studies in which the effect of HCl and acetic acid were respectively investigated, there is a lack of understanding of how the product is affected by changes in synthesis parameters.(4b, 5) It is especially important to attain such knowledge on UiO MOFs given that past studies(4d, 5, 6) have demonstrated there to be several ways in which a given UiO-66 sample may differ from the idealized, nondefective material of composition $Zr_6O_4(OH)_4(BDC)_6$. The most dramatic way that a sample may deviate from ideality is that it may have a significantly lower thermal stability than expected, an issue which has not been previously reported. Figure 1 (discussed in depth later) demonstrates the surprisingly wide variation in the thermal stabilities of three UiO-66 samples synthesized at different temperatures, highlighting how severely the material can be affected by alterations to the synthesis conditions.

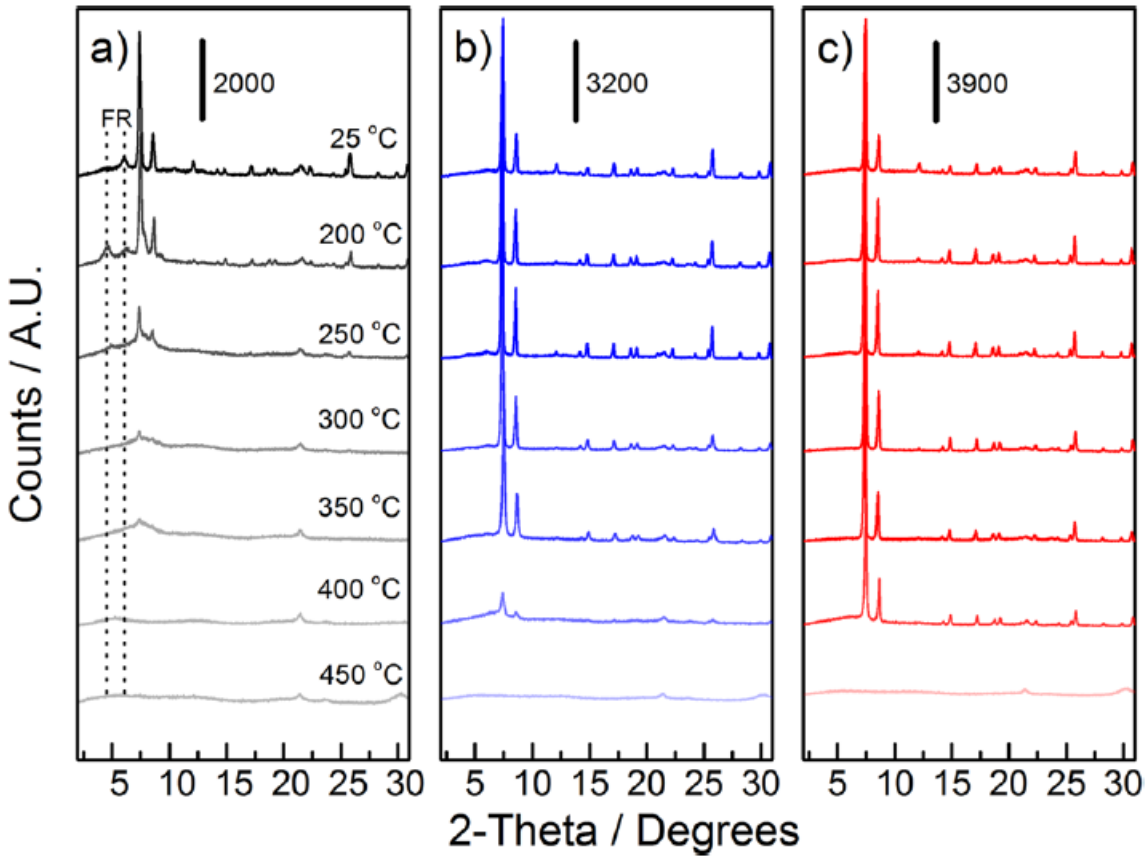

Figure 1. PXRD patterns recorded after heating UiO-66 samples for 12 h in air at various temperatures (indicated on part a of the figure). (a) Black curves, UiO-66-100-2:1-2DMF; (b) blue curves, UiO-66-160-2:1-2DMF; (c) red curves, UiO-66-220-2:1-2DMF. The two reflections labeled "FR" and traced by vertical dotted lines are symmetry forbidden.

In addition to poor thermal stability, we identify six ways in which a UiO-66 sample may deviate from what may be considered "ideal" for the material: (1) Symmetry forbidden reflections may appear in its PXRD pattern,(7) (2) its weight loss during thermal decomposition in air may be less than expected,(8) (3) its surface area may be much higher than theoretically expected,(4b) (4) its FTIR spectrum may contain multiple O–H stretching bands,(4b, 9) (5) it may contain chlorine,(6, 9) and (6) some bands in its Raman spectrum may be unexpectedly split and the fingerprints (<500 cm^{-1}) weakened. An "ideal" UiO-66 sample would exhibit none of these six characteristics.

The goal of this work is to understand the link between some of the major synthesis parameters and the physicochemical properties of the product and to find a method which affords an "ideal" sample, something which has not yet been demonstrated. To this end, we have found that, above all others, a method previously employed by Serre and co-workers(10) reproducibly yields a robust product with high thermal stability. Two features of this procedure stand out: (1) the use of 220 °C as the synthesis temperature and (2) an excess of BDC is added such that the BDC:Zr molar ratio in solution is 2:1. This differs from most other synthesis procedures in which the synthesis temperature is typically limited to 90–120 °C and BDC is added to the synthesis mixture in a 1:1 stoichiometric ratio with Zr.(2, 11) With the aim of elucidating why the former method produces

a superior UiO-66 product, we have synthesized and characterized a systematic series of samples in which three different synthesis temperatures (100, 160, and 220 °C) and five different BDC:Zr ratios (1:1, 5:4, 3:2, 7:4, and 2:1) were used. Moreover, the effect of DMF washing and methanol exchange procedures has been assessed. Samples are hereafter labeled by the formula "UiO-66-*x*-L:M-*y*" where *x* = synthesis temperature, L:M = BDC:Zr ratio, and *y* describes the extent of washing (blank = unwashed, 2DMF = washed twice in DMF, MeOH = methanol exchanged after two DMF washes). See the Supporting Information for full synthesis and washing details. All samples were extensively characterized, with particular emphasis on determining the extent to which the seven highlighted issues are present throughout the series.

The results displayed in Figure 1 were obtained on (a) UiO-66-100-2:1-2DMF, (b) UiO-66-160-2:1-2DMF, and (c) UiO-66-220-2:1-2DMF by heating them (1 °C/min ramp in a muffle furnace) to the indicated temperature where they were held for 12 h in air before being allowed to cool to room temperature for PXRD measurement. The use of such a long equilibration time allows the thermal stability of the materials to be reliably determined. See section C of the Supporting Information for discussion of the thermal stability tests on the full series of samples.

Returning attention to the figure, it can be seen that the thermal stability of UiO-66 is dramatically and systematically improved by increasing the synthesis temperature. The PXRD pattern of UiO-66-100-2:1-2DMF is already somewhat affected by treatment at only 200 °C. Significant crystallinity, however, is not lost until 250 °C, with a 300 °C heat treatment being required for amorphization. Treatment at this temperature typically resulted in 70% of the original sample mass being retained. Such a small weight loss is generally indicative of only solvent loss, suggesting that UiO-66-100-2:1-2DMF (and all other samples which are destroyed by low temperature treatments) has not collapsed dramatically as a result of burning the organic linkers but has simply rearranged into an amorphous material. Increasing the synthesis temperature to 160 °C affords a product which fairs significantly better. It begins to lose a small amount of crystallinity at 300 °C before amorphization at 400 °C. Finally, a synthesis temperature of 220 °C yields a UiO-66 sample which retains near perfect crystallinity until it decomposes at 450 °C. Only ca. 30% of the sample mass remains after treatment at this temperature, suggesting that the linkers were burned off, resulting in complete structure collapse. Since the burning of the organic fragments is unavoidable, we conclude that UiO-66-220-2:1 likely exhibits the maximum thermal stability attainable for UiO-66.

Regarding the other synthesis parameters investigated, we found that the BDC:Zr ratio had little effect on the thermal stability of the materials, while stability decreased with increasing extent of washing (see section C of the Supporting Information for more details). These further observations allowed us to discover that there is a strong correlation between poor thermal stability and the extent to which two weak and broad symmetry forbidden reflections (indexing to the (100) and (110) of a primitive cell) are evident in the low angle region of the PXRD pattern (see section D of the Supporting Information for more on this issue). Like thermal stability, their prominence does not vary significantly or systematically with the BDC:Zr ratio used in the synthesis. However, they are found to be increasingly prominent in samples which were (1) synthesized at lower temperatures (e.g., Figure 1a, where the reflections are emphasized by dotted lines), and (2) increasingly thoroughly washed. In a previous study on Hf-UiO-66, the symmetry forbidden reflections were attributed to disordered solvent molecules.(7a) However, one would not expect

such an assignment to account for significantly lowering the thermal stability of the host framework. A more satisfying assignment is provided by Cliffe and Goodwin,(7b) who recently performed an in depth study on how these reflections manifest in the PXRD pattern of Hf-UiO-66. They conclude that the reflections are due to extended defective regions intergrown with the regular framework. The regions are of composition $Hf_6O_4(OH)_4(BDC)_4(HCOO)_4$, which has a lower BDC:cluster ratio (= 4) than bulk UiO-66 (= 6), allowing them to be considered as "ordered" missing linker defects. Note that poor thermal stability is found only on samples in which forbidden reflections are evident and that samples without the reflections are stable even if they are linker deficient (see, e.g., sample UiO-66-160-1:1, Figures S10 and S79 in the Supporting Information).

Missing linker defects are commonly studied by thermogravimetric analysis (TGA).(6, 8) Their presence was first evidenced by considering the chemical equation for the aerobic decomposition of (dehydroxylated) UiO-66, $Zr_6O_6(BDC)_6$

$$Zr_6O_6(BDC)_6(s) + 45O_2(g) \rightarrow 6ZrO_2(s) + 48CO_2(g) + 12H_2O(g)$$

The molecular weight of $Zr_6O_6(BDC)_6$ is a factor of 2.2 higher than $6ZrO_2$, the only solid product. Thus, if the end weight of an aerobic TGA run is normalized to 100%, then the plateau (representing the empty, solvent free material) should ideally reach 220%. However, it typically falls significantly short of the theoretical weight, meaning that the framework is lighter than that formulated by the idealized equation. This observation led to the original hypothesis that some of the linkers are missing from the framework.(4b, 6, 8, 11) The presence of missing linker defects has recently been validated by neutron diffraction experiments(5) as well as discoveries of new zirconium MOFs in which there are less than 12 linkers per node.(12) However, due to the assumptions involved, the use of TGA for the study of such defects has recently come under criticism.(5) This controversy is opposed by the results in the current work.

The TGA-DSC curves of UiO-66-100-1:1-MeOH, UiO-66-100-2:1-MeOH, UiO-66-160–2:1-MeOH, and UiO-66-220-2:1-MeOH are presented in Figure 2a. TGA-DSC results for the rest of the materials in the series are presented and analyzed in detail in sections E and K3 of the Supporting Information. Starting the discussion with UiO-66-100-1:1-MeOH (gray curve), it can be seen that its TGA plateau is significantly below the expected value (highlighted by a horizontal dashed line on the figure). However, increasing the linker concentration in the synthesis mixture such that the BDC:Zr ratio is 2:1 (black curve) results in the plateau increasing toward (but still not close to) ideality, indicating that more linkers have been inserted into the structure. The TGA plateau is in fact found to systematically increase with the BDC:Zr ratio used (1:1 < 5:4 < 3:2 < 7:4 < 2:1) at all three synthesis temperatures (see Figures S9–S11 in the Supporting Information).

The last two curves in the figure emphasize the effect of increasing the synthesis temperature. It can clearly be seen that the plateau increases as the synthesis temperature increases to 160 °C (blue curve) and again to 220 °C (red curve). Moreover, the TGA plateau of UiO-66-220-2:1 appears not only to have reached the ideal value but to have surpassed it. However, an additional, slow weight loss is observed, starting at ca. 260 °C and ending at around 360 °C, where a second plateau is reached, matching exactly the theoretical value. The second weight loss is concurrent with the appearance of an exothermic heat signal in the DSC curve (dashed red curve), peaking at around 350 °C. Further TGA studies (Supporting Information, section E) provide strongly convincing

evidence that this second weight loss step is due to the burning of "excess linkers", unbound BDC molecules which likely reside in the pores of the material. Their presence (also evident on UiO-66-160-2:1, blue curve) makes sense when considering that an excess of linker was added to the synthesis.

Although not displayed here, it is possible to burn off the excess linkers by thermal treatment in air at 350 °C. Such a treatment also removes the DMF molecules, yielding an empty ideal UiO-66 sample which is subsequently filled with atmospheric water (see DRIFTS results in section H of the Supporting Information). However, this procedure can only be applied to thermally stable materials. Thus, in order to obtain comparable N_2 sorption data, samples were first methanol exchanged so that they may all be activated via the same, mild (150 °C) pretreatment. Dissolution/liquid ^{1}H NMR results show that the exchange and activation procedures were highly efficient (see Supporting Information sections G and K4). The methanol exchange procedure did not compromise the crystallinity of the materials, but was found to lower the TGA plateau of some of the samples, an example of which being UiO-66-160-2:1 (blue curve), which actually attains the ideal plateau before washing (see Supporting Information Figure S13). We can offer no definite explanation for this at this time, but framework linker removal by hydrolysis is probable.

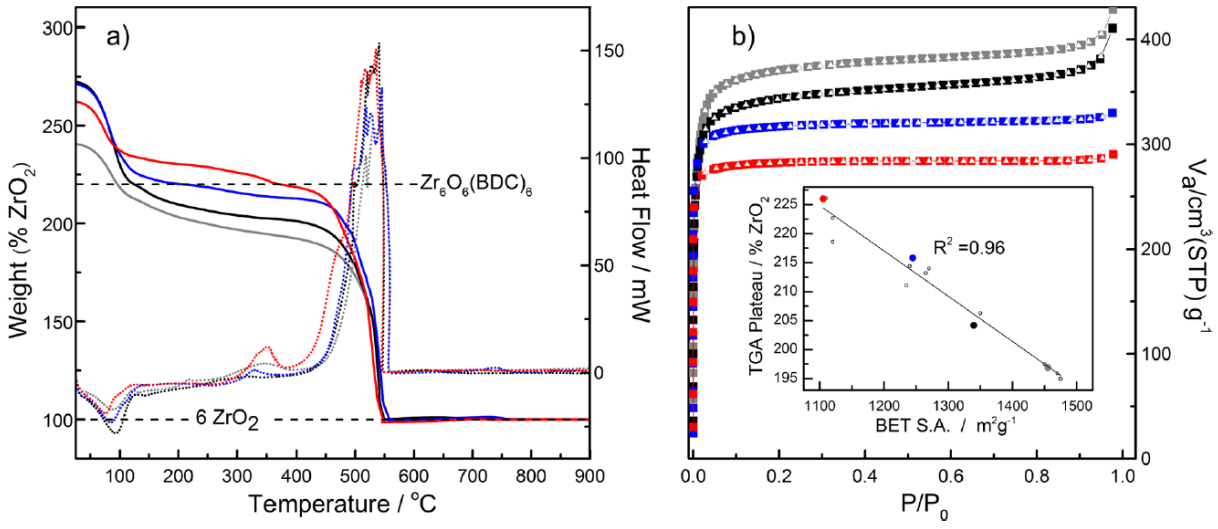

Figure 2. (a) TGA curves (relative to ZrO_2) in solid lines, DSC signals in dotted lines. (b) N_2 adsorption isotherms at 77 K, adsorption represented by filled squares, desorption by open triangles. Presented in the inset is the linear fit obtained when plotting the BET surface areas of all 15 materials against their respective TGA plateaus. Throughout the figure, data collected on UiO-66-100-1:1-CH_3OH, UiO-66-100-2:1-CH_3OH, UiO-66-160-2:1-CH_3OH and UiO-66-220-2:1-CH_3OH are displayed in gray, black, blue, and red, respectively.

Figure 2b displays the N_2 adsorption–desorption isotherms obtained on the same materials discussed in Figure 2a. The isotherms and resulting BET surface areas for the rest of the series are available in section F of the Supporting Information. From the figure, one can see that the nitrogen adsorption capacity varies significantly depending on synthesis conditions, resulting in BET surface areas ranging from 1105 (UiO-66-220-2:1) to 1455 (UiO-66-100-1:1) $m^2\ g^{-1}$. The BET surface area of UiO-66-220-2:1 is in very good agreement with that obtained via N_2 adsorption isotherms simulated on an ideal model of the UiO-66 structure (1125 $m^2\ g^{-1}$), again emphasizing the ideality of the sample. Moreover, the trend in nitrogen uptake is the inverse of that seen for the

TGA plateaus of the materials. This makes sense if one accepts the hypothesis that a lower TGA plateau is indicative of a more linker deficient and hence more porous framework. This inverse relation is observed over the entire series of 15 samples, such that a very good linear fit is obtained when their TGA plateaus are plotted against their respective BET surface areas (Figure 2b, inset). Further results obtained from simulated nitrogen adsorption isotherms (Supporting Information, section F) show that the relationship between the number of linker vacancies and the BET surface area is in fact also linear, providing strong evidence that the controversial(5) "missing linker" interpretation of TGA is solid.

Until now it has been unclear what missing linkers are replaced by, meaning that the exact quantity of these defects cannot be determined by TGA without first making assumptions. The ways in which the defects have previously been suggested to be compensated are by formate(7b, 12b) (via the decomposition of DMF), oxide,(13) hydroxide, water, or chloride.(4b, 9) Moreover, monocarboxylic acids can compensate linker deficiencies when heavily modulated synthesis procedures are used (not relevant here).(5, 6, 12a) Within this series of samples, formate has been ruled out as it was not observed in the dissolution/liquid ^{1}H NMR spectra (Supporting Information, sections G and K4) of the materials after methanol exchange. Hydroxide and water have also been ruled out as only the expected single O–H band was observed in the DRIFTS spectrum (Supporting Information, Figure S18) of not only UiO-66-220-2:1 (again indicating the ideality of this sample) but also the highly linker deficient UiO-66-100-5:4. Our elemental analyses (by EDS, Supporting Information section I) instead infer that chloride may partially (if not fully) compensate linker deficiencies in our samples, many of which contain significant amounts even after thorough washing. UiO-66-220-2:1, on the other hand, is once again found to exhibit ideal behavior, being chlorine free after two DMF washes. Samples with lower TGA plateaus (such as those synthesized at 100 °C) were generally found to have higher chlorine content, consistent with the idea that chloride compensates for missing linkers. This is highly plausible provided that MOF formation likely proceeds via sequential hydrolysis of $ZrCl_4$ by linker carboxylate groups. One can envision that incomplete hydrolysis would result in the formation of a linker deficient framework in which vacancies are terminated by chloride.

As a final piece of highly convincing evidence for the ideality of UiO-66-220-2:1, its Raman spectrum was found to compare remarkably well with that simulated (via periodic DFT) from an ideal model of UiO-66 (see Supporting Information, section J). UiO-66-100-1:1, however, deviates significantly, particularly in regions associated with the carboxylate groups and cluster, as may be expected of a linker deficient material.

To conclude, this thorough systematic study has demonstrated the dramatic yet logical impact that the synthesis conditions can have on the properties of UiO-66. Seven potential pitfalls regarding sample ideality were investigated, affording the conclusion that the material systematically becomes more "ideal" when the BDC:Zr ratio and/or synthesis temperature are increased. Such gravitation toward ideality makes sense when one notes that linker deficiencies are the underlying cause of the majority of pitfalls. We suggest that increasing the synthesis temperature and/or BDC:Zr ratio shifts the solution equilibrium in favor of BDC-Zr bonds, aiding the "ironing out" of linker deficiencies. This approach ultimately yields "ideal" UiO-66 with unsurpassed thermal stability when the synthesis is performed with a 2:1 BDC:Zr ratio at 220 °C.

Supporting Information

Details of synthesis/washing and details of/data from the following: thermal treatments/PXRD, TGA-DSC, N_2 adsorption isotherms (experimental and simulated), dissolution/liquid ^1H NMR, DRIFTS, EDS, and Raman (experimental and simulated). This material is available free of charge via the Internet at http://pubs.acs.org.

§Author Present Address

Southern Federal University, Zorge Street 5, 344090 Rostov-on-Don, Russia.

The authors declare no competing financial interest.

Acknowledgment

Lorenzo Maschio is acknowledged for the simulated Raman spectrum. MIUR-PRIN 2010-2011 and The Research Council of Norway are kindly acknowledged for economic support via Projects 2010A2FSS9 and 174893, respectively. Computer time was provided by the NOTUR Project NN4683K. C.L. acknowledge the Mega-grant of the Russian Federation Government at Southern Federal University, No. 14.Y26.31.0001.

References

(1) (a) Yaghi, O. M.; O'Keeffe, M.; Ockwig, N. W.; Chae, H. K.; Eddaoudi, M.; Kim, J. Nature 2003, 423, 705. (b) Kitagawa, S.; Kitaura, R.; Noro, S. Angew. Chem., Int. Ed. 2004, 43, 2334. (c) Ferey, G. Chem. Soc. Rev. 2008, 37, 191.

(2) Cavka, J. H.; Jakobsen, S.; Olsbye, U.; Guillou, N.; Lamberti, C.; Bordiga, S.; Lillerud, K. P. J. Am. Chem. Soc. 2008, 130, 13850.

(3) Eddaoudi, M.; Kim, J.; Rosi, N.; Vodak, D.; Wachter, J.; O'Keeffe, M.; Yaghi, O. M. Science 2002, 295, 469.

(4) (a) Biswas, S.; Van der Voort, P. Eur. J. Inorg. Chem. 2013, 2154. (b) Katz, M. J.; Brown, Z. J.; Colon, Y. J.; Siu, P. W.; Scheidt, K. A.; Snurr, R. Q.; Hupp, J. T.; Farha, O. K. Chem. Commun. 2013, 49, 9449. (c) Ragon, F.; Horcajada, P.; Chevreau, H.; Hwang, Y. K.; Lee, U. H.; Miller, S. R.; Devic, T.; Chang, J.-S.; Serre, C. Inorg. Chem. 2014, 53, 2491. (d) Schaate, A.; Roy, P.; Godt, A.; Lippke, J.; Waltz, F.; Wiebcke, M.; Behrens, P. Chem.-Eur. J. 2011, 17, 6643.

(5) Wu, H.; Chua, Y. S.; Krungleviciute, V.; Tyagi, M.; Chen, P.; Yildirim, T.; Zhou, W. J. Am. Chem. Soc. 2013, 135, 10525.

(6) Vermoortele, F.; Bueken, B.; Le Bars, G.; Van de Voorde, B.; Vandichel, M.; Houthoofd, K.; Vimont, A.; Daturi, M.; Waroquier, M.; Van Speybroeck, V.; Kirschhock, C.; De Vos, D. E. J. Am. Chem. Soc. 2013, 135, 11465.

(7) (a) Jakobsen, S.; Gianolio, D.; Wragg, D. S.; Nilsen, M. H.; Emerich, H.; Bordiga, S.; Lamberti, C.; Olsbye, U.; Tilset, M.; Lillerud, K. P. Phys. Rev. B 2012, 86, 125429. (b) Cliffe, M.; Goodwin,

A. Presented at EUROMAT-2013 European Congress and Exhibition on Advanced Materials and Processes, Sevilla, 2013.

(8) Valenzano, L.; Civalleri, B.; Chavan, S.; Bordiga, S.; Nilsen, M. H.; Jakobsen, S.; Lillerud, K. P.; Lamberti, C. Chem. Mater. 2011, 23, 1700.

(9) Shearer, G. C.; Forselv, S.; Chavan, S.; Bordiga, S.; Mathisen, K.; Bjorgen, M.; Svelle, S.; Lillerud, K. P. Top. Catal. 2013, 56, 770.

(10) Barcia, P. S.; Guimaraes, D.; Mendes, P. A. P.; Silva, J. A. C.; Guillerm, V.; Chevreau, H.; Serre, C.; Rodrigues, A. E. Microporous Mesoporous Mater. 2011, 139, 67.

(11) Kandiah, M.; Nilsen, M. H.; Usseglio, S.; Jakobsen, S.; Olsbye, U.; Tilset, M.; Larabi, C.; Quadrelli, E. A.; Bonino, F.; Lillerud, K. P. Chem. Mater. 2010, 22, 6632.

(12) (a) Bon, V.; Senkovska, I.; Weiss, M. S.; Kaskel, S. CrystEngComm 2013, 15, 9572. (b) Furukawa, H.; Gándara, F.; Zhang, Y.-B.; Jiang, J.; Queen, W. L.; Hudson, M. R.; Yaghi, O. M. J. Am. Chem. Soc. 2014, 136, 4369. (c) Morris, W.; Volosskiy, B.; Demir, S.; Gandara, F.; McGrier, P. L.; Furukawa, H.; Cascio, D.; Stoddart, J. F.; Yaghi, O. M. Inorg. Chem. 2012, 51, 6443.

(13) Vermoortele, F.; Vandichel, M.; Van de Voorde, B.; Ameloot, R.; Waroquier, M.; Van Speybroeck, V.; De Vos, D. E. Angew. Chem., Int. Ed. 2012, 51, 4887.